Received: 4 October 2023 | Revised: 5 February 2024 | Accepted: 18 February 2024

DOI: 10.1002/ajpa.24926

RESEARCH ARTICLE

AMERICAN JOURNAL OF BIOLOGICAL ANTHROPOLOGY
The Official Journal of the American Association of Biological Anthropologists

WILEY

Masticatory habits of the adult Neanderthal individual BD 1 from La Chaise-de-Vouthon (France)

María Hernaiz-García[1] | Clément Zanolli[2] | Laura Martín-Francés[3,1] | Arnaud Mazurier[4] | Stefano Benazzi[5] | Rachel Sarig[6,7] | Jing Fu[8] | Ottmar Kullmer[9,10] | Luca Fiorenza[1]

[1]Monash Biomedicine Discovery Institute, Department of Anatomy and Developmental Biology, Monash University, Melbourne, Australia

[2]Univ. Bordeaux, CNRS, MCC, PACEA, Pessac, France

[3]Department of Paleobiology, CENIEH, Burgos, Spain

[4]CNRS, Institut de Chimie des Milieux et Matériaux de Poitiers-IC2MP, Université de Poitiers, Poitiers, France

[5]Department of Cultural Heritage, University of Bologna, Ravenna, Italy

[6]Department of Oral Biology, The Goldschleger School of Dental Medicine, Sackler Faculty of Medicine, Tel Aviv University, Tel Aviv, Israel

[7]Dan David Center for Human Evolution and Biohistory Research, Sackler Faculty of Medicine, Tel-Aviv University, Tel Aviv, Israel

[8]Department of Mechanical and Aerospace Engineering, Monash University, Melbourne, Australia

[9]Division of Palaeoanthropology, Senckenberg Research Institute and Natural History Museum Frankfurt, Frankfurt am Main, Germany

[10]Department of Palaeobiology and Environment, Institute of Ecology, Evolution, and Diversity, Goethe University, Frankfurt, Germany

Correspondence
María Hernaiz-García Biomedicine Discovery Institute, Department of Anatomy and Developmental Biology, Monash University, Melbourne, Victoria, Australia.
Email: maria.hernaizgarcia@monash.edu

Funding information
Biomedicine Discovery Scholarship from Monash University; Australian Research Council, Grant/Award Number: DP190100465

Abstract

Objectives: The analysis of dental wear provides a useful approach for dietary and cultural habit reconstructions of past human populations. The analysis of macrowear patterns can also be used to better understand the individual chewing behavior and to investigate the biomechanical responses during different biting scenarios. The aim of this study is to evaluate the diet and chewing performance of the adult Neanderthal Bourgeois-Delaunay 1 (BD 1) and to investigate the relationship between wear and cementum deposition under mechanical demands.

Materials and methods: The macrowear pattern of BD 1 was analyzed using the occlusal fingerprint analysis method. We propose a new method for the bilateral measurement of the cementum volume along both buccal and lingual sides of the molar root.

Results: BD 1's anterior dentition is more affected by wear compared to the posterior one. The macrowear pattern suggest a normal chewing behavior and a mixed-diet coming from temperate environments. The teeth on the left side of the mandible display greater levels of wear, as well as the buccal side of the molar crowns. The cementum analysis shows higher buccal volume along the molar roots.

Discussion: BD1 could have been preferably chewing on the left side of the mandible. The exploitation of various food resources suggested by the macrowear analysis

is compatible with the environmental reconstructions. Finally, the greater wear on the buccal side of the molar occlusal surface and the greater volume of cementum in that side of the molar roots offers a preliminary understanding about the potential correlation between dental wear and cementum deposition.

KEYWORDS
biomechanics, dental macrowear, diet, ecology, occlusal fingerprint analysis

1 | INTRODUCTION

Dental wear has been extensively studied for dietary and cultural habits reconstructions (El Zaatari et al., 2016; Estalrrich et al., 2017; El Zaatari & Hublin, 2014; Fiorenza et al., 2011; Fiorenza, Benazzi, & Kullmer, 2011; Fiorenza, 2015; Molnar, 1972) and for the virtual simulation of the masticatory behaviors in human fossils (Fiorenza et al., 2011; Fiorenza & Kullmer, 2013; Kullmer et al., 2009). More specifically, the analysis of tooth wear at the macroscopic scale has been used to reconstruct the diet and cultural habits of Neanderthals (Fiorenza, 2015; Fiorenza et al., 2015, 2018, 2019, 2020; Fiorenza et al., 2011; Fiorenza & Kullmer, 2013) which, in combination with isotopic analyses (Naito et al., 2016; Salazar-García et al., 2013) and study of dental calculus (Hardy et al., 2012; Henry et al., 2011; Salazar-García et al., 2013), confirmed that this species relied on a broader dietary spectrum than previously thought.

BD 1 is a fossil mandible with complete and well-preserved dental crowns with moderate degree of wear that belonged to a Neanderthal individual of 20–35 years of age (Condemi, 2001). This specimen was recovered in 1967 from the layer 12 of Abri Bourgeois-Delaunay cave shelter located in the final Middle to initial Late Pleistocene site complex of La Chaise-de-Vouthon (Southwestern France) (Debénath, 1967). BD 1 has been dated between 127 and 116 ka (MIS 5e) (Debénath, 2006) and was found in association with faunal remains (Armand, 1998) and pollen of plant species (Blackwell et al., 1983; David & Prat, 1965) corresponding to temperate environments. The current study aims to investigate the diet and cultural habits of the specimen BD 1, as well as its chewing behavior, through the analysis of tooth macrowear patterns. This can be evaluated by the application of the Occlusal Fingerprint Analysis (OFA) method (Kullmer et al., 2009; Kullmer et al., 2020), which allows the identification and characterization of the occlusal wear to interpret the masticatory mechanisms, diet and possible cultural behaviors (Fiorenza, 2015; Fiorenza et al., 2018; Fiorenza et al., 2019; Fiorenza et al., 2011; Fiorenza et al., 2011; Fiorenza & Kullmer, 2013; Kullmer et al., 2009). Based on faunal remains (cave lions, hyenas, wolves, foxes, cave bears, bovids, cervids, and horses) and palynological data (hazel, ash, and beech) recovered from the Abri Bourgeois-Delaunay layer of occupation and based on the interglacial landscape characterized by the vegetal cover proliferation of coniferous and Mediterranean forest tree species (van Andel & Tzedakis, 1996) associated to BD 1's chronology (Debénath, 2006), we expect to find a dental macrowear pattern similar to those of Pleistocene humans living in temperate deciduous environments, who exploited plant and animal food resources (Fiorenza et al., 2011).

Zanolli et al. (2020) study on BD 1 reported a slight right dominance in cortical bone thickness distribution at the molar level. However, this previous study did not quantify the extent and distribution of tooth wear in BD 1, and in-depth analyses of the variation of dental tissues with respect to occlusal wear patterns remain to be done following a systematic approach as previously determined for the Neanderthal mandible of Regourdou 1 (Fiorenza et al., 2019). Thereby, we will combine BD 1's macrowear data with the cementum volume of the molars to obtain information on how biomechanics affects dental wear (Kullmer et al., 2009) and tissue distribution (Nanci, 2007). In the specific case of Neanderthals, dental biomechanics was firstly discussed on the light of their large and heavily worn incisors and canines (Rak, 1986; Smith, 1982). Moreover, the labially convex and lingually concave surface of the root of Neanderthal's anterior dentition, together with thicker dentine layer along that surface compared to *Homo sapiens*, have also been interpreted as an adaptation to sustain high biomechanical demands (Le Cabec et al., 2013). Measurements of dental cementum in paleontological material are generally taken using cross-sections of the roots at the cervical, mid-height, and apical thirds levels, and by quantification of the total volume (Grine et al., 2023; Le Cabec et al., 2013; Martinón-Torres et al., 2011). In this study, we aim to quantify the cementum volume along the buccal and lingual sides of the molar roots in order to evaluate if larger levels of tooth wear on the buccal or lingual aspect of the crown correlate with greater cementum deposition on each side of the root. Cementum undergoes continuous remodeling throughout life (Bosshardt & Selvig, 2000; Hillson, 2001). Its deposition variation has been related to the compensatory mechanism of continuous eruption, and it was also related to high levels of dental wear (Hillson, 2001). Nevertheless, non-functioning/impacted teeth generally appear to have thicker cementum than functioning teeth (Azaz et al., 1974; Bailey & Hublin, 2006). Moreover, other factors such as periodontal diseases can stimulate cementum deposition and eventually lead to hypercementosis (Brooks et al., 2019; Martinón-Torres et al., 2011; Zhou et al., 2012). Cementum covers the outer surface of the dentine along the root and helps in providing support by reducing stress concentration during biting (Bosshardt & Selvig, 2000; Ren et al., 2010). While acellular cementum is mainly implicated in tooth structure attachment of the Sharey's fibers of the periodontal ligament (PDL) in the alveolar process and it distributes along the coronal two-thirds of the root (Bosshardt & Selvig, 2000; Nanci, 2007), cellular cementum has been

hypothesized to develop in response to masticatory loadings and is located in the apical third of the root (Bosshardt & Selvig, 2000; Morgenthal et al., 2021; Nanci & Bosshardt, 2000; Rios et al., 2008). A previous biomechanical study described highest stress occurring on the root during intrusive forces, which was greatest on the cementum layer (if compared to PDL and alveolar bone) (Shaw et al., 2004). This is probably associated to the cementum tissue composition, which is also the least mineralized (Ho et al., 2004; Ho et al., 2007). The lower mineral content implies lower mechanical properties (Ho et al., 2010; Shaw et al., 2004), which helps in reducing and in absorbing the mechanical stress (Ren et al., 2010). During mastication, the PDL is subjected to compressive, tensile, and shearing forces which trigger both collagen degradation (due to compression) and collagen synthesis (due to tension) within its fibrous matrix (Krishnan & Davidovitch, 2009). Periodontal ligament transformation entails simultaneous remodeling of cementum since it contains precursor cells of cementoblasts (involved in cementogenesis) (Bousnaki et al., 2022; Consolaro et al., 2012). Periodontal ligament over-compression may reduce the rate of cement deposition (Bosshardt & Selvig, 2000), whereas the cementoblasts are activated by cyclic stretch stimuli (Rego et al., 2011). The progressive cementum thickening reduces tooth bending and it decreases the maximal tensile stress of tooth structure (Morgenthal et al., 2021). Because thicker cementum layer has been found at the buccal side of the roots in modern human mandibular molars (Nicklisch et al., 2023), we hypothesize that greater volumes of cementum should be observed along BD 1 buccal side of the roots, which, in turn, could also be accompanied by a greater level of wear.

TABLE 1 Dentine exposures areas (mm^2) and wear scores (Smith, 1984) of BD 1's mandibular teeth.

Tooth	Side	Dentine area	Wear score
I_1	R	7.26	5
I_1	L	8.53	5
I_2	R	6.87	5
I_2	L	6.37	5
C_1	R	5.85	4
C_1	L	3.75	3
P_3	R	2.05	3
P_3	L	2.28	3
P_4	R	1.74	3
P_4	L	0.19	2
M_1	R	11.62	3
M_1	L	13.13	4
M_2	R	1.44	3
M_2	L	5.85	3
M_3	R	0.52	2
M_3	L	1.47	2

Abbreviations: L, left; R, right.

2 | MATERIALS AND METHODS

2.1 | Models acquisition

Three-dimensional (3D) digital models of molars were obtained from surface scans of dental casts, while 3D models of anterior teeth and premolars derived from micro-CT data. Firstly, the original dentition was molded using a light viscosity polyvinylsiloxane silicone, Provil Novo Light C.D.2 (Heraeus Kulzer GmbH). Dental replicas were created using a special gypsum (EverestH Rock, KaVo) with non-reflective properties and optimized for 3D scanning (Fiorenza et al., 2009). Finally, 3D digital models were generated using a blue LED light scanning system (Artec Micro 3D) with a resolution of 29 µm. The acquisition and alignment of the scan-data point clouds was carried out using Artec Studio 15 Professional (Artec Micro 3D). Regarding the micro-CT data collection, BD 1 fossil was scanned at the European Synchrotron Radiation Facility of Grenoble, in France (experiment SC1587c), according to the following parameters: energy, 70 keV; projections, 1500 in half acquisition mode; integration time, 22.9 ms. The synchrotron data were reconstructed to a voxel size of 45.5 µm.

We used a comparative human fossil sample published in Fiorenza et al. (2011), where Neanderthals and anatomically modern humans (AMH) were grouped into three eco-geographical groups (deciduous woodland, Mediterranean evergreen and steppe/coniferous forest), based on chronology, vegetation reconstruction (van Andel & Tzedakis, 1996), and bibliographical information about fauna and pollen data (SI, Table 1). The casts of the comparative sample were digitized using a white light scanning system with a resolution of 55 µm (smartSCAN 3D, Breuckmann GmbH) (Fiorenza et al., 2011). The differences in the scanner resolution may lead to differential decimation rates (reduction of the total amount of polygons in a mesh while preserving the original geometry) (Friess, 2012). However, decimation of dental surfaces was not found to affect the characterization of small features while assessing molar topography of different sized teeth (Skinner et al., 2010). Moreover, the study of relative wear facet areas, and not of absolute dimensions, should further minimize measurement discrepancies between 3D scans characterized by different resolutions. The use of high-resolution digital models can help to better identify the wear facets onto the 3D polygonal surface of a tooth. However, for wear facet identification we also used high-resolution dental casts and high-quality photos taken from the original specimens. Thus, we expect to find negligible difference in wear facet identification between 3D scans of slightly different resolutions.

2.2 | Occlusal fingerprint analysis

The post-processing of the digital scans was carried out in PolyWorks® V12.1 (InnovMetric Software Inc.), a 3D model editing software (SI, Figure 1). The orientation of each 3D model was carried out in the IMEdit module of PolyWorks® V12.1 by creating a reference

plane (cervical plane) (Kullmer et al., 2009). Subsequently we manually outlined the occlusal wear facets and dentine exposures into the 3D models' surface following the labeling system created by Maier and Schneck (1981) and later modified by Kullmer et al. (2009) (Figure 2a). The wear facets consist on the flat and polished surface resulting from the worn enamel and not including the dentine exposures, which are delimited and characterized separately. For each wear facet we calculated its area, inclination and direction. Both the inclination and the direction were obtained in the IMInspect module of PolyWorks® V12.1. The inclination was obtained by calculating the angle between the facet plane and reference plane, while for the direction we used the occlusal compass, obtained by translating and projecting the normal vector of each facet into the reference plane (Figure 2b) (Kullmer et al., 2009).

Furthermore, we grouped the occlusal wear facets based on chewing cycle phases (Fiorenza et al., 2011; Janis, 1990; Kay & Hiiemae, 1974) (Figure 3): Buccal Phase I (facets 1, 2, 2.1, 3, and 4), Lingual Phase I (facets 5, 5.1, 6, 6.1, 7, and 8) and Phase II (facets (9, 10, 11, 12 and 13) (Figure 3). Finally, the wear stage was assessed for each BD 1's teeth according to Smith (1984) methodology.

FIGURE 1 BD 1 mandible. Photography: Luca Fiorenza.

2.3 | Cementum volume distribution

We measured the cementum volume deposition along the buccal and lingual aspects of the molar roots. Due to the lack of studies assessing the bilateral distribution of the cementum, here we present a new method to generate a mesio-distal plane that allows bilateral measurements within the tooth structure (Figure 4). The central groove is a typical feature of hominin molar crowns (Hillson, 2003) and it has been used to delimit buccal and lingual molar cusps in previous morphometric analyses (Gómez-Robles et al., 2011, 2015; Martinón-Torres et al., 2013). Gómez-Robles et al. (2015) employed four homologous landmarks along the central groove placed at the following anatomical points: 1. anterior fovea, 2. intersection between central and mesio-buccal grooves, 3. intersection between central and lingual grooves; 4. intersection between central groove and distobuccal grooves. Due to molar size reduction and morphological variability along the molar row (Kieser, 1990), we located equidistant semilandmarks

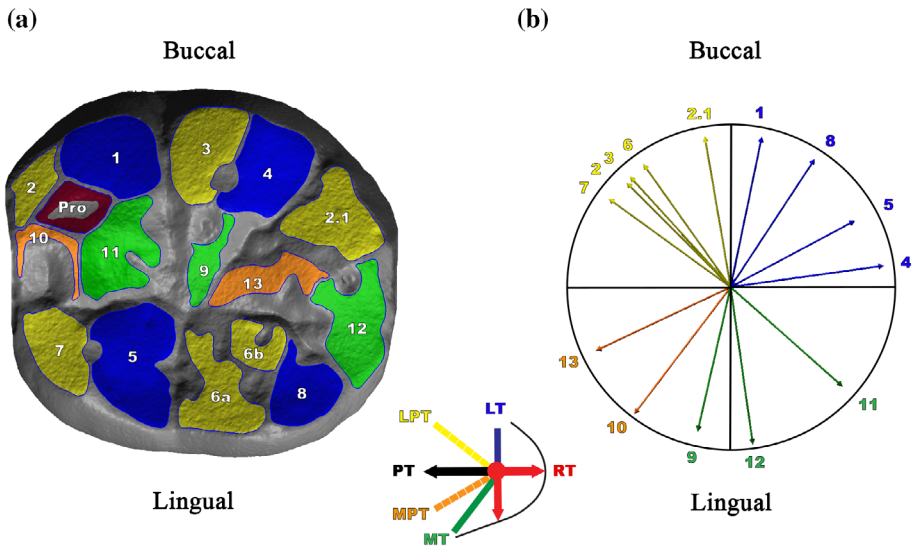

FIGURE 2 (A) Occlusal wear facets of BD 1 RM_2. The color code is based on the dental occlusal concept (Douglass & DeVreugd, 1997; Kullmer et al., 2009). (B) Occlusal compass of BD 1 RM_2 showing the direction and inclination of all facet vectors schematizing the lower jaw movements. The central image corresponds to the mandibular direction of possible occlusal movements behind wear facet formation. Facets 1, 4, 5, 5.1 and 8 form during lateroretrusive movements (LRT; in blue); facets 2, 2.1, 3, 6, 6.1 and 7 are produced by lateroprotrusion (LRT, in yellow); facets 9, 11 and 12 start developing during mediotrusion (MT, in green) and immediate side shift (ISS, in red.) motion; and facets 10 and 13 contact when medioprotrusive movements occur (MPT, in orange). The dark red area corresponds to the facet developing around the tip of the protoconid as a consequence of tip-crushing actions.

among points 1 and 4 for first and second molars, and among points 2 and 4 for third molars. Together with the landmarks positioned along the central groove, a single landmark was placed in the apex of the distal root to define the mesio-distal cutting plane (Figure 4.1). A cervical plane was generated by several equidistant landmark location along the cervical line (Figure 4.1) in order to remove the crown of the molars (Figure 4.2). Finally, both buccal and lingual root sides were isolated (Figure 4.4). Aiming to ensure an equitable allocation of the radicular tissues the dentine volume was measured so to check that both buccal and labial volumes were similar. The calculation of the Average Cementum Thickness (ACT) was based on the modified AET (Average Enamel Thickness) in Olejniczak et al. (2008). The 3D models were processed in Avizo® V2021.2. The 3D occlusal surface area of each molar is also provided as a dimensional value for the contextualization of the side-based comparison of cementum volumes. The 3D occlusal area was calculated by selecting the triangles of the 3D polygonal model above the occlusal plane (Fiorenza et al., 2023; Harty et al., 2022). The occlusal plane was obtained by translating the reference (or cervical) plane along the *z* axis until it reached the deepest point on the occlusal surface.

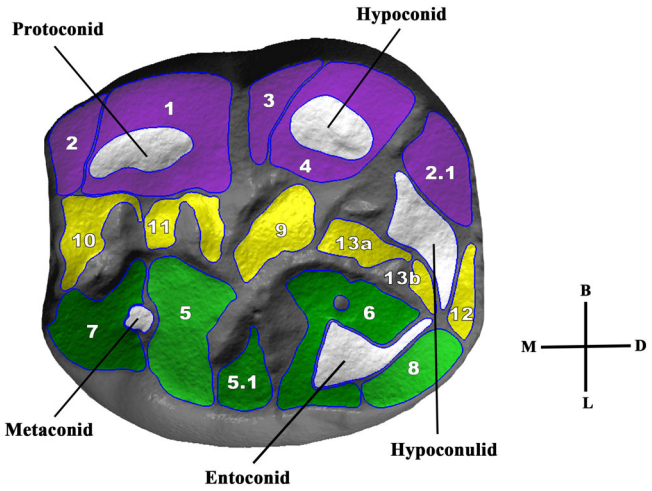

FIGURE 3 Occlusal wear pattern of the Neanderthal right M_1 of BD 1. 3D virtual model showing the dentine exposures (in white) and the wear facets divided into Buccal Phase I facets (purple), Phase II facets (yellow), and Lingual Phase I facets (green). Numbering based on Kullmer et al. (2009). Orientation: buccal (B), mesial (M), lingual (L), distal (D).

2.4 | Statistical analysis

BD 1 molar macrowear pattern was compared to an available dataset of Neanderthal and AMH specimens from a previous study where the fossil sample was grouped into three different biomes (deciduous woodland, Mediterranean evergreen and steppe/coniferous forest) (Fiorenza et al., 2011). For BD 1, we selected the RM_2 for comparative purpose with the already analyzed Neanderthal mandible of Regourdou 1 (Fiorenza et al., 2019). The visual representation is depicted in a ternary plot, which is a diagram showing the proportions of three different variables within a triangle where each of the sides represent a scale from 0 to 100%. In this study case, the variables represented are the Buccal Phase I, Lingual Phase II and Phase II facets. The ternary plot was created using the software PAST v4 (PAlaeontological STatistics) (Hammer & Harper, 2006).

In order to analyze the masticatory behavior of BD 1 we employed circular statistical methods (Fiorenza et al., 2019; Fiorenza et al., 2011; Fiorenza & Kullmer, 2013, 2016). The facet's directions have been reported by the following descriptive parameters: mean angle, circular standard deviation and 95% confidence interval. We also calculated the concentration parameter κ to assess the normal distribution of the circular data. This variable measures the amount of data comprised between two standard deviation values. The largest κ value is, the larger sample size follows a normal distribution (Fisher, 1993). The Rayleigh's and Rao's tests allow to evaluate if the sample follows specific directions or if it is randomly distributed (Fisher, 1993). The visual representations of the facet's major directions were depicted by using rose diagrams, where data frequency and orientation are shown (Robson, 1994). Directional statistical results and rose diagrams were obtained in Oriana™ v. 4.00 (Kovach Computing Services, Pentraeth, UK).

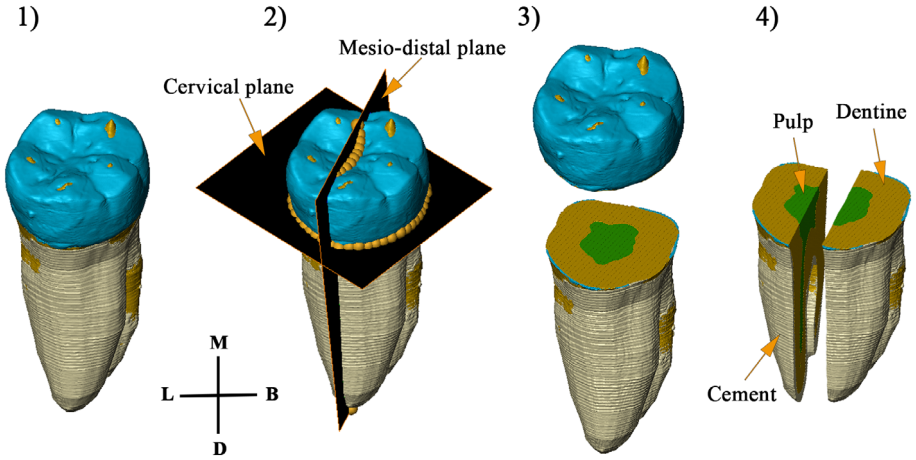

FIGURE 4 (1) BD 1 RM_2. (2) Cervical plane and mesio-distal plane definition by landmarks. (3) Crown and root separation. (4) Buccal and lingual root side division for cementum volume measurement. Orientation: buccal (B), mesial (M), lingual (L), distal (D).

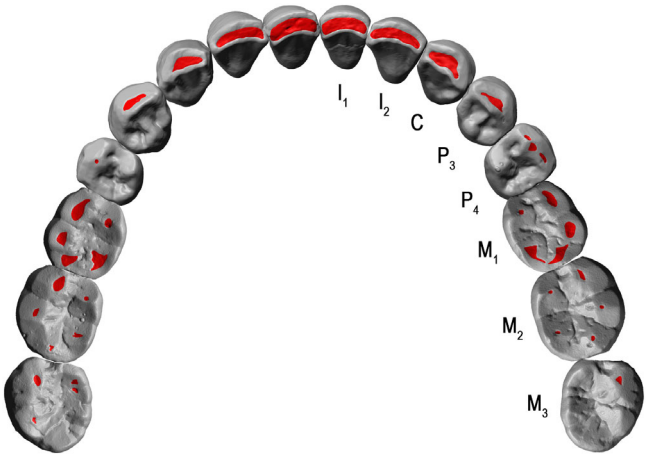

FIGURE 5 Dentine exposures (highlighted in red) of the BD 1 mandible in occlusal view.

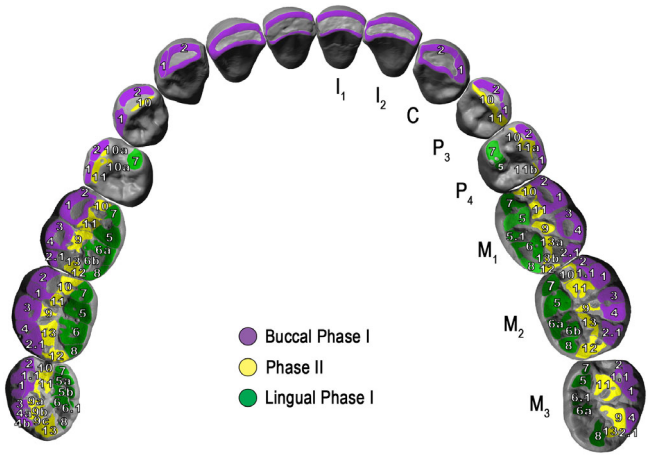

FIGURE 6 Dental macrowear analysis showing the different wear facets grouped by chewing cycle phases (Kay & Hiiemae, 1974): Buccal Phase I wear facets, Phase II wear facets, and Lingual Phase I wear facets.

TABLE 2 Posterior dentition enamel wear (mm^2) and dentine exposures areas (mm^2) grouped together by buccal and lingual cusps.

		Enamel wear		Dentine exposures	
Tooth	Side	Buccal	Lingual	Buccal	Lingual
P_3	R	10.45	0	2.05	0
P_3	L	13.24	0	2.30	0
P_4	R	9.20	5.20	1.54	0.20
P_4	L	8.30	3.93	0.19	0
M_1	R	32.70	21.80	8.00	3.70
M_1	L	39.90	26.00	8.30	4.80
M_2	R	42.00	20.70	1.10	0.40
M_2	L	50.70	26.70	5.00	0.80
M_3	R	26.30	23.80	0.50	0
M_3	L	37.60	21.80	1.00	0.40

Abbreviations: L, left; R, right.

TABLE 3 Relative wear facet areas (in %) of left and right molars of the Neanderthal BD 1 mandible.

Tooth	Buccal	Lingual	Phase II
R M_1	0.40	0.40	0.20
L M_1	0.36	0.40	0.24
R M_2	0.40	0.35	0.25
L M_2	0.41	0.35	0.24
R M_3	0.36	0.21	0.43
L M_3	0.36	0.30	0.34

Abbreviations: L, left; R, right.

3 | RESULTS

3.1 | Occlusal fingerprint analysis

The anterior teeth of BD 1 mandible show a greater level of wear compared to the posterior dentition (Table 1), with larger dentine exposures (Figure 5). The incisors exhibit a flat dentine exposure area along the incisal edge surrounded by a worn enamel rim. Tooth wear appears to be more pronounced on the central incisors than on the lateral ones. The canines display a similar wear pattern, but the worn area is divided into two planes with different inclinations: a flat one on the incisal edge and a second one located on a steep distolabial facet. The flat facets display a dentine exposure surrounded by enamel wear, whereas the steep facets do not show any dentine exposures.

Regarding the postcanine dentition, the dentine exposures tend to be moderate and decrease distally from M_1 to M_3. Third premolars exhibit greater dentine exposures than fourth premolars, in the same way that dentine exposure size decreases from first molars toward third molars. This has an impact on the occlusal surface of the molars leading to a flatter occlusal morphology in first molars and more pronounced cusps' slopes in second and third molars. The comparison between right and left molars rows reveals that the left side of the mandible is characterized by a slightly greater level of wear. Regarding premolars, there is no clear asymmetry in relation to wear (Table 2).

The first molars show the most advanced wear of all postcanine dentition. Well-developed and independent dentine areas are visible in the five main cusps of both M_1s. The dentine exposure on the entoconid nearly coalesces with the hypoconulid one on the right M_1 generating a dentine concavity and leading to a flatter distal portion of the crown. Although still significant, dental wear in M_2s is less developed than in M_1s, showing regular-shaped wear facets (Figure 6) with discrete dentine exposures on each cusp, apart from the protoconid one which is still moderate. Protoconid continues to be the cusp most affected by wear in M_3s while the rest of the cusps exhibit small or even absent dentine exposures. There is no dental wear in the distal portion of the right M_3 entoconid.

Buccal Phase I facets tend to be the most developed among almost all molars (Table 3). Overall, the presence of advanced wear stages it is

not accompanied by flatter facet inclination (Table 4). There is a lack of correlation between the level of wear and the facet inclination. Only M_3s represent an exception: the greater level of wear of Phase II tie in with flatter facet planes (in right M_3), and higher values of wear for Buccal Phase I facets match the flatter surface for those areas (in left M_3).

3.2 | Ecogeographic analysis

For the comparative analysis of relative wear facet areas, we used the right M_2 of BD 1, which is characterized by 40% of Buccal Phase I facets, 35% of Lingual Phase I facets and 25% of Phase II areas (Table 5).

By representing these values on a ternary diagram (in which each phase grades from 0% to 100%), BD 1 plots within the distribution range of Neanderthals and AMH associated to temperate climates dominated by deciduous woodland landscapes (DEW group; Figure 6, in green) and separated to those attributed to steppe/coniferous forests (SCF; Figure 7, in blue) and Mediterranean evergreen (MED; Figure 7, in orange).

3.3 | Major occlusal movements

Circular statistical analysis of BD 1 lower molars and premolars represented in the rose diagrams (Figure 8) confirm that all major occlusal movements fall within a von Mises distribution due to the large κ values. Moreover, lateroprotrusive, lateroretrusive and medioprotrusive movements displayed preferred directions, with statistically significant values ($p < 0.05$) for Rayleigh's and Rao's tests. The mediotrusive/immediate side shift movement seems to display a random distribution since neither Rayleigh's test nor Rao's spacing tests provide with statistically significant values (Table 6).

3.4 | Cementum thickness and 3D occlusal surface area

Volumetric analyses (Table 7; SI, Table 2) performed on the roots of BD 1 molars reveal that radicular dentine volume shows similar values

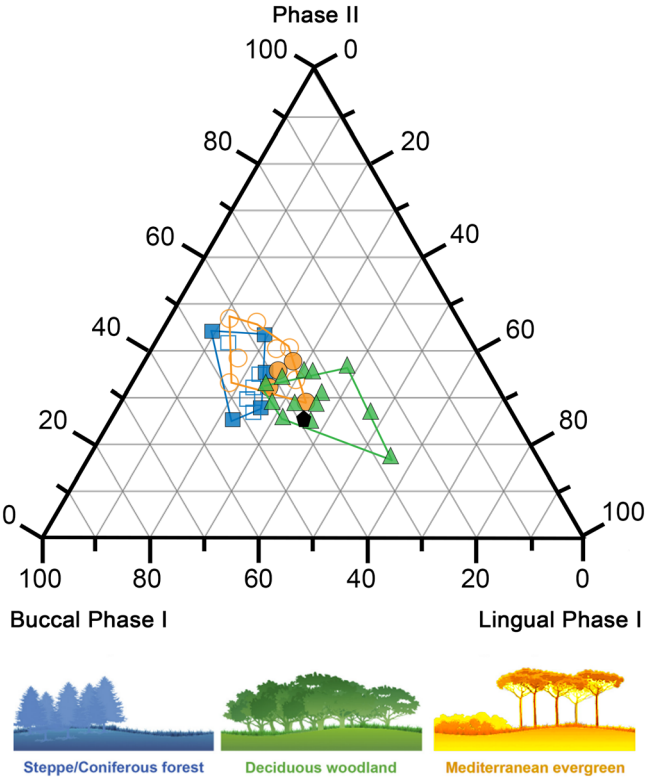

FIGURE 7 Ternary diagram showing the proportions (in %) of relative wear areas of Buccal Phase I facets, Lingual Phase I facets, and Phase II facets of BD 1 right M_2. BD 1 is represented by a black pentagone. Its wear pattern is compared to published data of upper molars (Fiorenza, 2015; Fiorenza et al., 2011), where Neanderthals (filled symbols) and AMH (open symbols) were grouped into three distinct ecogeographical contexts: steppe/coniferous forest (SCF, blue squares), deciduous woodland (DEW, green triangles), and Mediterranean evergreen (MED, orange circles).

TABLE 4 Wear facet inclinations (in °) of left and right molars of the Neanderthal BD 1 mandible.

Tooth	Buccal	Lingual	Phase II
R M_1	18.11	23.40	11.75
L M_1	9.53	17.94	14.63
R M_2	18.95	22.78	18.85
L M_2	22.53	23.14	21.64
R M_3	30.31	27.44	19.83
L M_3	12.18	23.13	19.85

Abbreviations: L, left; R, right.

TABLE 5 Descriptive statistics of relative wear facet areas (in %) within the fossil biome groups and BD 1 individual. Data for the three ecogeographic groups (steppe/coniferous forest, deciduous woodland and Mediterranean evergreen) are from Fiorenza (2015) and Fiorenza et al., 2011. Groups: DEW = Deciduous woodland; MED = Mediterranean evergreen; SCF = Steppe/coniferous forest.

		Buccal phase I		Lingual phase I		Phase II	
Groups/specimens	*n*	Mean	SD	Mean	SD	Mean	SD
DEW	13	37	5.3	34.3	8.8	28.8	4.7
MED	11	39.3	4	23.2	6.7	37.5	5.6
SCF	11	45	3.8	20.6	5	34.4	5.8
BD 1	1	40	–	35	–	25	–

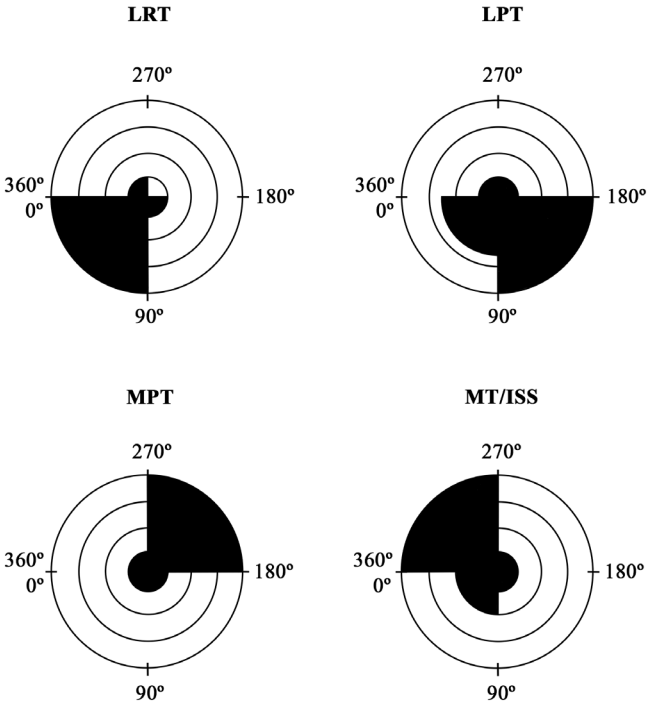

FIGURE 8 Circular rose diagrams generated in Oriana 4 software (Kovach Computing Services) and representing the directions and frequency of each occlusal movement: LRT (lateroretrusion); LPT (lateroprotrusion); MPT (medioprotrusion); MT/ISS (mediotrusion/immediate sideshift).

in both buccal and lingual sides. The dentine surface area of the lingual side of the root is smaller compared to the buccal side. Therefore, all three molar type exhibit greater lingual ACT. The bilateral comparison reports the ACT to be higher in the right M_1, right M_3 and in the left M_2. The 3D occlusal surface area displays larger values for both right M_2 and M_3 and left M_1.

4 | DISCUSSION

4.1 | Chewing behavior

The macrowear distribution observed in BD 1 follows the typical Neanderthal pattern, with incisors and canines displaying a more advanced wear stage compared to the posterior dentition. This condition has been long-established as an association to the use of the anterior dentition as a tool (Fiorenza et al., 2020; Molnar, 1972; Smith, 1982; Trinkaus, 1992; Wolpoff, 1971). Overall, the left dentition of BD 1 is the most affected by wear. This asymmetric macrowear pattern could tell us about the chewing preferences of this individual, as previously highlighted by other studies (Fiorenza et al., 2019; Khamnei et al., 2019; Lamontagne et al., 2013). Nonetheless, Diernberger et al. (2008) found no correlation between asymmetric wear facets and an asymmetric chewing behavior. This opens the possibility that asymmetry of the masticatory apparatus could have also played a role in the appearance of an uneven wear pattern (Oxilia et al., 2018) which, in turn, could impact the dietary interpretations. Oxilia et al. (2018) found no statistically significant differences between right and left macrowear pattern in mandibular molars. However, we should not rule out the possibility that antagonistic contacts, affected by asymmetric tooth inclination, could also influence the wear pattern distribution. This is based on the lack of correlation between tooth inclination of opposed dental arches (Oxilia et al., 2018). The asymmetry of the maxilla and mandible could change the ratio of Buccal Phase I/Lingual Phase I facets which, in case of significant differences, might lead to the perception of a meat-based diet (larger Buccal Phase I facets) or a vegetable-preferred diet (larger Lingual Phase I facets) (Fiorenza et al., 2011).

It is worth mentioning that although dental tissue proportions are equally distributed between the left and the right antimeres without a clear asymmetric pattern, a slight right dominance in cortical bone

Facets	Mean	SD	κ	95%	Rayleigh (*p*)	Rao (*p*)
LPT	114.1	59.9	1.3	–	**0.03**	0.50 > p > 0.10
LRT	58.5	36.2	2.2	32.3–84.7	**0.0003**	**<0.01**
MPT	236.9	58.4	1.4	–	**0.025**	**<0.05**
MT/ISS	299.1	69.8	0.88	–	0.13	0.50 > p > 0.10

TABLE 6 Basic circular statistic parameters measured for the major occlusal movements' directions in BD 1 posterior dentition. Significant values ($p < 0.05$) are highlighted in bold.

TABLE 7 Three-dimensional cementum thickness measurements.

	Vcem (mm^3)		Vd (mm^3)		Sd (mm^2)		ACT (mm)		
Tooth	Buccal	Lingual	Buccal	Lingual	Buccal	Lingual	Buccal	Lingual	3D occlusal surface area (mm^2)
LLM1	63.35	65.59	277.47	279.59	435.66	294.14	0.15	0.22	117.68
LRM1	71.80	105.58	224.33	222.39	355.20	263.17	0.20	0.40	102.38
LLM2	66.20	58.67	282.24	285.56	403.00	262.58	0.16	0.22	126.48
LRM2	71.56	59.02	330.14	292.06	476.96	289.22	0.15	0.20	138.71
LLM3	29.01	27.77	262.78	189.09	366.68	184.22	0.08	0.15	109.27
LRM3	71.47	68.69	245.84	164.69	362.52	188.29	0.20	0.36	116.31

Abbreviations: ACT, average cementum thickness; Sdent, radicular dentine area; Vcem, radicular cementum volume; Vd, radicular dentine volume.

thickness is found at M_1/M_2 and M_2/M_3 levels (Zanolli et al., 2020). The discrepancy between asymmetric wear and cortical bone distribution, similar to that observed in Regourdou 1 (Fiorenza et al., 2019), could be partially due to the balancing movements that occur in the non-working side of the mandible during mastication, since not every mandibular strain during the chewing cycle necessarily correlates with reaction forces along the dentition (Hylander & Crompton, 1986). In fact, the mandible is subjected to maximum load before reaching centric occlusion (Buccal Phase I phase of the power stroke) (Hylander & Crompton, 1986). Moreover, it has been proved that humans use relatively greater amount of balancing-side muscle force when chewing foodstuff of increasing toughness (Hylander, 1979b, 1983). Therefore, if BD 1 had a mixed diet, it would not be surprising to find bilateral asymmetries in cortical bone distribution along the mandibular corpus (Zanolli et al., 2020).

Wear is affecting the occlusal morphology of posterior dentition in a different way depending on tooth position, the mesially-located teeth being the more worn in each tooth type. Overall, the evaluation of each of BD 1's posterior tooth macrowear patterns reveals that the buccal aspect of the crowns appears to exhibit the greatest level of wear, which are associated with shearing movements during mastication (Kay, 1975a, 1975b; Kay & Hiiemae, 1974). It is especially remarkable that Phase II areas of the right M_3 exhibit the greatest value for this tooth, which could be due to its buccally-oriented mesial region of the crown. This orientation would have prevented a normal occlusion situation, making the lingual cusps of the right M^3 to have greater contacts with the lower molar basin.

The directional data suggests that the macrowear patterns observed in BD 1's postcanine teeth are formed during a normal chewing behavior, in spite of the random distribution of MS/ISS movements. Such variation might be related to the flat morphology of the central portion of the crown, which allows a wider range of movements between opposing teeth (; Anders et al., 2011; Fiorenza et al., 2011; Maier & Schneck, 1981).

4.2 | Diet

The molar macrowear analysis of BD 1 indicates that this specimen could have had a diet consisting of both meat and vegetable foodstuff. A previous study based on the macrowear assessment of upper molars' macrowear pattern found dominantly that meat-eating populations exhibited great Buccal Phase I facets compared to the more developed Lingual Phase I facets of mixed-diet human groups (Fiorenza et al., 2011). In spite of the difference in tooth class between the comparative sample and BD 1, the wear pattern distribution between the upper and lower molars is not expected to be considerably different. The study of Zanolli et al. (2019) showed a more similar macrowear pattern of upper and lower molars for modern humans and Neanderthals compared to apes, which perform greater lateral motion during chewing (Hylander, 1979a). Moreover, Oxilia et al. (2018) compared the macrowear patterns of upper and lower molars of an Australian Aboriginal population finding no statistically significant differences. Therefore, the fact that BD 1's macrowear pattern displays almost equally values for Buccal Phase I and Lingual Phase I facets could be associated to a mixed-diet.

The conception of Neanderthal as top predators with little variation through time and space (Bocherens et al., 2005; Richards & Trinkaus, 2009) has gradually changed toward a population with a varied diet. While the majority of isotopes studies suggest a carnivorous diet for these human group (Bocherens, 2011; Bocherens et al., 2005; Jaouen et al., 2022; Richards & Trinkaus, 2009), some others point at a vegetal supplement when the environmental conditions allowed it (Naito et al., 2016; Salazar-García et al., 2013). In fact, dental calculus samples belonging to Neanderthal individuals revealed that their diet also contained plant materials (Hardy et al., 2012; Henry et al., 2011; Salazar-García et al., 2013).

More specifically, dental microwear investigations have been effective in distinguishing between Neanderthals from cold open environments, who tend to mainly rely on the consumption of meat, and those from wooded environments, who also include plant material (El Zaatari et al., 2011; El Zaatari et al., 2016; Estalrrich et al., 2017). This has been also corroborated by occlusal macrowear studies in Neanderthal specimens that have been associated to a mixed-diet (Fiorenza et al., 2015; Fiorenza et al., 2019; Fiorenza et al., 2011).

In the particular case of BD 1, the wear pattern of its right M_2 is within the range of variation of individuals inhabiting deciduous woodland ecosystems. This is consistent with the macrofaunal and floral species recovered at the Abri Bourgeois-Delaunay site, and that is associated to temperate environments (Armand, 1998; Blackwell et al., 1983; David & Prat, 1965). The chronology of BD 1 places that individual between 127 and 115 ka, period linked to the MIS 5e (Debénath, 2006) and characterized by mild climatological conditions related to the interglacial event Riss/Würm (Debénath, 1967). During the last interglacial event the ice-sheets covering the northern regions of Europe started to melt, the sea level rose reaching levels similar to those of nowadays and trees spread over the open landscapes in Europe (van Andel & Tzedakis, 1996). The vegetal succession began with the appearance of deciduous *Quercus*, *Ulmus* and *Corylus*, followed by the progression of coniferous evergreen species, such as *Picea*, *Pinus* or *Taxus*, and Mediterranean forest characterized by *Olea* and evergreen oak (van Andel & Tzedakis, 1996). The changing habitats in Europe provided with new resources to many other Neanderthals who, like BD 1, inhabited the deciduous woodland ecosystems and relied on the intake of mixed food resources thanks to the abundance of edible vegetable materials coming from the wooded environments (Fiorenza, 2015; Fiorenza et al., 2019; Fiorenza et al., 2011).

Differing from the interglacial environmental conditions of the OIS 5e that BD 1 lived in (Debénath, 2006), the OIS 4 was overall characterized by a gradual climate deterioration after OIS 5 with a major ice advance in Europe around 65 ka (van Andel & Tzedakis, 1996). This was the environmental frame for the Neanderthal individual Regourdou 1 (Plavcan et al., 2014). However, the faunal remains in the layer of occupation of Regourdou 1 and the palaeoclimatological reconstructions of the zone suggest a mild phase within OIS 4 when this specimen could have also enjoyed warm ecological

conditions (Bonifay et al., 2007; Nicholson, 2017; Plavcan et al., 2014). The animal remains associated to Regourdou 1 consist of bovids, cervids, bears, suids, leporids and castors (Vandermeersch & Trinkaus, 1995). This wildlife entails similarities with the one gathered at the Abri Bourgeois-Delaunay, where cave lions, hyenas, wolves, fox, cave bears, bovids, cervids and horses have been found (Armand, 1998). These faunal affinity makes it feasible that both Neanderthals, BD 1 and Regourdou 1, were exploiting animal resources within their respective habitats. In fact, the study of Dodat et al. (2021) analyzed the calcium isotopic composition from bone sample of Regourdou 1 finding a low $\delta^{44/42}$Ca values, which is generally associated to the consumption of meat. Yet, Tacail et al. (2019) suggested close values of $\delta^{44/42}$Ca for meat and plant consumption. This reinforces the data obtained from the macrowear analysis that found similar percentages of Buccal Phase I facets (30%) and Lingual Phase I facets (38%) for Regourdou 1 (Fiorenza et al., 2019), respectively associated to carnivorous and mixed-dietary habits (Fiorenza et al., 2011). For this reason, the similar pattern found in BD 1 (40% of Buccal Phase I facets and 35% of Lingual Phase I facets) along with the findings of hazel, ash and beech associated to the specimen (Blackwell et al., 1983; David & Prat, 1965) are now interpreted as evidence for having a mixed-diet favored by the moderate climatological conditions of the interstadial event OIS 5e (Debénath, 1967, 2006).

4.3 | Cementum thickness

Our findings show greater cementum volume depositions along the lingual side of the molar roots compared to the buccal counterpart. Larger Buccal Phase I facets developed on the occlusal surface of BD 1 posterior dentition, which may indicate that cementum development could not be necessarily correlated to dental wear but more associated to the distribution of mechanical loads during the chewing cycle.

Considering that mastication likely occurs more frequently on the left side of BD 1's mandible, the less biomechanical pressure on the right side during the individual's life could be related to the higher total cementum volume on the right molars of BD 1 (Azaz et al., 1974; Bailey & Hublin, 2006), along with thicker cortical bone on this side (Zanolli et al., 2020). When evaluating both cementum and cortical bone more in detail, they seem to provide with thicker tissue under the same regions within the left side of the mandible and presents asymmetry on the right side. Zanolli et al. (2020) pointed at the thicker cortical bone on the lingual side of the mandibular corpus in the preferential side of mastication and on the buccal aspect of the mandible in the non-preferred side. Cementum volume appears to be greater on the lingual aspect of the molar roots of both mandible sides. Therefore, the lingually-located distribution of cementum could be more related to the strain's distribution pattern along the tooth and surrounding tissues rather than to wear. Considering the working side of the mandible during a normal chewing activity, the mandibular corpus mainly undergoes twisting forces along its long axis (Hylander, 1979a). While, the muscle force tends to evert the lower edge of the mandible and invert the alveolar process, the bite force twists the mandible in the opposite direction, everting the alveolar process and inverting the lower mandibular border (Hylander, 1979a). Benazzi et al. (2016) considered the dynamic simulation of occlusal loads during a normal chewing cycle in a modern human lower molar. They reported that tensile stress increases in the alveolar portion of the mandible, mainly in the lingual side. In addition, the tensile stress concentrated along the buccal side of the PDL (Benazzi et al., 2016). Tension has been hypothesized as the driving mechanism for cementum secretion (Ho et al., 2010; Rego et al., 2011), hence the findings of thicker cementum layer along the buccal side of the modern humans' mandibular molars (Nicklisch et al., 2023) agrees with previous studies. However, BD 1 shows the opposite pattern with more cementum volume deposition over the lingual side of the mandibular molar's root. This variation could be due to: 1. different measurements comparison. Nicklisch et al. (2023) measured the thickness of the cementum in a transverse section of the root at its cervical third, which could be disregarding the whole cementum distribution. Since tensile stress distributes differently along the entire PDL length depending on the occlusal loading conditions (Benazzi et al., 2016), the cementum thickness may vary accordingly. Consequently, the volumetric measurements of the cementum on both root sides provides a more comprehensive understanding about this tissue's behavior; 2. differences in mandibular strain locations between Neanderthals and modern humans during mastication due to their distinct craniomandibular architecture (Stringer & Gamble, 1993). Although, prognathism has been associated to greater stress under several facial regions in modern humans (Patriquin, 2013), its relation to dental stress distribution is still unknown. Further investigations need to be performed in order to assess the possible masticatory differences between Neanderthals and modern humans.

When comparing lingual cementum deposition between left and right molars, the results are uneven. Even if left molars are more worn than the right ones, their wear pattern does not match with greater cementum volumes in the lingual side of the root for every molar. In fact, only the left M_2 appears to exhibit greater cementum volume compared to its right antimere. M_1 is the first reaching occlusion during ontogeny, which means that its chewing activity has taken place for longer compared to M_2 and M_3, thus, increased mechanical demands (Morgenthal et al., 2021). The larger wear of the left M_1, linked to greater occlusal loads (Edmonds & Glowacka, 2020; Kullmer et al., 2009), could have entailed PDL over-compression compared to its antimere, which has been suggested as a factor that may reduce cementum deposition (Bosshardt & Selvig, 2000). Moreover, the more advanced wear stages reduce tooth topography favoring wider range of occlusal movements (Hylander, 1983) along with a more variable stress dispersion due to the change in loading directions (Benazzi et al., 2013) and reduction in tooth tilting (Morgenthal et al., 2021). This, could have led to a more variable cementum volume deposition along the roots of M_1s. Zanolli et al. (2020) reported greater total cementum volume in right molars. Nevertheless, the differences between antimeric molars were minimal for M_1s and M_2s, whereas

right M_3 presented more than double the cementum volume of the left M_3. The lateral orientation of the right M_3 might have influenced load distributions favoring cementum secretion and, eventually, leading to a non-reliable comparison between the cementum volume measurements along the buccal and lingual aspects for this tooth. The 3D occlusal surface data shows that molar dimensions seem not to be linked to the side-based difference in cementum volume deposition. Right M_3 represents the only exception to this since it shows greater 3D occlusal surface and lingual cementum volume compared to its counterpart. However, due to the increasing intra-observer error when measuring cementum volumes in M_3s compared to M_1s and M_2s (SI, Table 2) which, in turn, could be affected by the morphological variability along the molar row (Kieser, 1990), we prefer to remain cautious with our interpretations. Future studies analyzing larger samples will help in better understanding the relation between tooth size and dental tissue development.

Overall, BD 1 shows a distinct pattern of cementum volume distribution along the molar roots characterized by greater lingually-located accumulation compared to modern humans. Future biomechanical studies based on accurate masticatory loading scenarios along with mandibular tissues structure, can help to reveal whether different anatomical configurations in Neanderthals could lead to this difference.

The principal limitation of this work is that we only studied a few individuals. Future studies will need to increase the sample size to better understand the Neanderthal chewing behavior and diet. This links with the second limitation of our study, which refers to the inference of BD 1's diet in comparison to upper molar macrowear data. Future studies should consider the wider variability in terms of tooth type and populations which could help in accurately assessing diet in relation to lower molar macrowear. Besides, the use of a broader mandibular sample would provide important information to understand the complexity of the strain patterns along the human mandible (Ichim et al., 2007) and their relation to dental wear and tissue remodeling. It is important to note that this study does not differentiate between acellular and cellular cementum, therefore we should consider our results as preliminary. It has been hypothesized that only cellular cementum responds to masticatory loadings (Bosshardt & Selvig, 2000; Morgenthal et al., 2021; Nanci & Bosshardt, 2000; Rios et al., 2008). Future studies differentiating between both cementum types will provide more accurate insights into tooth adaptation in relation to occlusal activity. Moreover, dental macrowear could also be integrated with kinematic simulations of the chewing cycle as well as with finite element analyses. The occlusal movements' simulation enables the detection of the contact areas between antagonistic teeth for the posterior incorporation in the finite element models (Benazzi et al., 2011). The accurate loading conditions in high resolution finite element models will help evaluating the biomechanical performance of the mandibular system (Benazzi et al., 2012; Benazzi et al., 2013; Benazzi et al., 2016; Fiorenza et al., 2015) to interpret the relationship between macrowear patterns, mandibular anatomy and occlusal loadings.

AUTHOR CONTRIBUTIONS

María Hernaiz-García: Formal analysis (equal); methodology (equal); writing – original draft (equal). **Clément Zanolli:** Data curation (equal); writing – review and editing (equal). **Laura Martín-Francés:** Writing – review and editing (equal). **Arnaud Mazurier:** Data curation (equal); writing – review and editing (equal). **Stefano Benazzi:** Writing – review and editing (equal). **Rachel Sarig:** Writing – review and editing (equal). **Jing Fu:** Writing – review and editing (equal). **Ottmar Kullmer:** Writing – review and editing (equal). **Luca Fiorenza:** Conceptualization (equal); funding acquisition (equal); resources (equal); supervision (equal); writing – review and editing (equal).

ACKNOWLEDGMENTS

The fossil specimen BD 1 is curated at the Musée d'Angoulême. The scanning BD 1 mandible was performed within the framework of the European «TNT Project» at the ESRF beamline ID 17 (Grenoble) thanks to the local collaboration provided by A. Bravin, C. Nemoz, and P. Tafforeau. For contribution to the documentation and analysis of both fossils, we thank P. Bayle, A. Bergeret, L. Bondioli, F. Gröning, R. Macchiarelli, and V. Volpato. This study was supported by the Australian Research Council (grant number: DP190100465) and a Biomedicine Discovery Scholarship coming from Monash University. Laura Martín-Francés received funding from the Horizon Program-Marie Sklodowska-Curie Actions of the EU Ninth program (2021-2027) under the HORIZON-MSCA-2021-PF-01-Project: 101060482. Open access publishing facilitated by Monash University, as part of the Wiley - Monash University agreement via the Council of Australian University Librarians.

CONFLICT OF INTEREST STATEMENT

There are no conflicts of interest.

DATA AVAILABILITY STATEMENT

Access to data will be granted under the contact to the corresponding author.

ORCID

María Hernaiz-García https://orcid.org/0000-0002-0459-7276
Clément Zanolli https://orcid.org/0000-0002-5617-1613
Laura Martín-Francés https://orcid.org/0000-0001-5853-5014
Luca Fiorenza https://orcid.org/0000-0001-7110-3398

REFERENCES

Anders, U., von Koenigswald, W., Ruf, I., & Smith, B. H. (2011). Generalized individual dental age stages (IDAS) for fossil and extant placental mammals. *Paläontologische Zeitschrift*, *85*(3), 321–339.

Armand, D. (1998). La faune de la grotte Bourgeois-Delaunay, commune de La Chaise-de-Vouthon (Charente). *Résultats Préliminaires*, *10*, 77–86.

Azaz, B., Ulmansky, M., Moshev, R., & Sela, J. (1974). Correlation between age and thickness of cementum in impacted teeth. *Oral Surgery Oral Medicine Oral Pathology*, *38*, 691–694.

Bailey, S. E., & Hublin, J. J. (2006). Dental remains from the Grotte du Renne at Arcy-sur-cure (Yonne). *Journal of Human Evolution*, *50*, 485–508.

Benazzi, S., Kullmer, O., Grosse, I. R., & Weber, G. W. (2011). Using occlusal wear information and finite element analysis to investigate stress distributions in human molars. *Journal of Anatomy*, *219*, 259–272.

Benazzi, S., Kullmer, O., Grosse, I. R., & Weber, G. W. (2012). Brief communication: Comparing loading scenarios in lower first molar supporting bone structure using 3D finite element analysis. *American Journal of Physical Anthropology*, *147*, 128–134.

Benazzi, S., Nguyen, H. N., Kullmer, O., & Hublin, J. J. (2013). Unravelling the functional biomechanics of dental features and tooth wear. *PLoS One*, *8*, e69990.

Benazzi, S., Nguyen, H. N., Kullmer, O., & Kupczik, K. (2016). Dynamic modelling of tooth deformation using occlusal kinematics and finite element analysis. *PLoS One*, *11*, e0152663.

Blackwell, B., Schwarcz, H. P., & Debénath, A. (1983). Absolute dating of hominids and palaeolithic artifacts of the cave of La chaise-de-Vouthon (Charente), France. *Journal of Archaeological Science*, *10*(6), 493–513.

Bocherens, H. (2011). Diet and ecology of Neanderthals: Implications from C and N isotopes: Insights from bone and tooth biogeochemistry. In N. J. Conard & J. Richter (Eds.), *Neanderthal Lifeways, Subsistence and Technology: One Hundred Fifty Years of Neanderthal Study*. Dordrecht, Springer Netherlands.

Bocherens, H., Drucker, D. G., Billiou, D., Patou-Mathis, M., & Vandermeersch, B. (2005). Isotopic evidence for diet and subsistence pattern of the Saint-Césaire I Neanderthal: Review and use of a multi-source mixing model. *Journal of Human Evolution*, *49*, 71–87.

Bonifay, E., Vandermeersch, B., Couture, C., & Panattoni, R. (2007). La sepulture néandertalienne du Regourdou (Montignac-sur-Vézère, Dordogne). *Documents du Centre d'Etude et de Recherche sur les Lacs, Anciens Lacs et Tourbieres du Massif-Central*, *4*, 1–18.

Bosshardt, D. D., & Selvig, K. A. (2000). Dental cementum: The dynamic tissue covering of the root. *Periodontology*, *13*, 41–75.

Bousnaki, M., Beketova, A., & Kontonasaki, E. (2022). A review of in vivo and clinical studies applying scaffolds and cell sheet technology for periodontal ligament regeneration. *Biomolecules*, *12*, 435.

Brooks, J. K., Ghita, I., Vallee, E. M., Charles-Marcel, A. L., & Price, J. B. (2019). Florid hypercementosis synchronous with periodontitis: A case report. *Quintessence International*, *50*, 478–485.

Condemi, S. (2001). Les Néandertaliens de La Chaise. Paris: C.T.H.S.

Consolaro, A., Consolaro, R. B., & Francischone, L. A. (2012). Cementum, apical morphology and hypercementosis: A probable adaptive response of the periodontal support tissues and potential orthodontic implications. *Dental Press Journal of Orthodontics*, *17*, 21–30.

David, P., & Prat, F. (1965). Considérations sur les faunes de la Chaise (commune de Vouthon, Charente). Abris Suard et Bourgeois Delaunay. *Bulletin de l'Association Française pour l'Etude du Quaternaire*, *2*, 222–231.

Debénath, A. (1967). Découverte d'une mandibule humaine à la Chaise-de-Vouthon (Charente). *C.R. de l'Académie Des Sciences de Paris*, *265*, 1170–1171.

Debénath, A. (2006). *Néanderthaliens et Cro-Magnons. Les temps glaciaires dans le Bassin de la Charente*. Le Croît Vif.

Diernberger, S., Bernhardt, O., Schwahn, C., & Kordass, B. (2008). Self-reported chewing side preference and its associations with occlusal, temporomandibular and prosthodontic factors: Results from the population-based study of health in Pomerania (SHIP-0). *Journal of Oral Rehabilitation*, *35*, 613–620.

Dodat, P. J., Tacail, T., Albalat, E., Gómez-Olivencia, A., Couture-Veschambre, C., Holliday, T., Madelaine, S., Martin, J. E., Rmoutilova, R., Maureille, B., & Balter, V. (2021). Isotopic calcium biogeochemistry of MIS 5 fossil vertebrate bones: Application to the study of the dietary reconstruction of Regourdou 1 Neandertal fossil. *Journal of Human Evolution*, *151*, 102925.

Douglass, G. D., & DeVreugd, R. T. (1997). The dynamics of occlusal relationships. In C. McNeill (Ed.), *Science and practice of occlusion*. Quintessence Publishing Co.

Edmonds, H. M., & Glowacka, H. (2020). The ontogeny of maximum bite force in humans. *Journal of Anatomy*, *237*, 529–542.

El Zaatari, S., Grine, F. E., Ungar, P. S., & Hublin, J. J. (2011). Ecogeographic variation in Neandertal dietary habits: Evidence from occlusal molar microwear texture analysis. *Journal of Human Evolution*, *61*, 411–424.

El Zaatari, S., Grine, F. E., Ungar, P. S., & Hublin, J. J. (2016). Neandertal versus modern human dietary responses to climatic fluctuations. *PLoS One*, *11*, e0153277.

El Zaatari, S., & Hublin, J. J. (2014). Diet of upper Paleolithic modern humans: Evidence from microwear texture analysis. *American Journal of Physical Anthropology*, *153*, 570–581.

Estalrrich, A., El Zaatari, S., & Rosas, A. (2017). Dietary reconstruction of the El Sidrón Neandertal familial group (Spain) in the context of other Neandertal and modern hunter-gatherer groups. A molar microwear texture analysis. *Journal of Human Evolution*, *104*, 13–22.

Fiorenza, L. (2015). Reconstructing diet and behaviour of Neanderthals from Central Italy through dental macrowear analysis. *Journal of Anthropological Sciences*, *93*, 113.

Fiorenza, L., Benazzi, S., Estalrrich, A., & Kullmer, O. (2020). Diet and cultural diversity in Neanderthals and modern humans from dental macrowear analyses. In C. W. Schmidt & J. T. Watson (Eds.), *Dental wear in evolutionary and biocultural contexts*. Academic Press.

Fiorenza, L., Benazzi, S., & Kullmer, O. (2009). Morphology, wear and 3D digital surface models: Materials and techniques to create high-resolution replicas of teeth. *Journal of Anthropological Sciences*, *87*, 211–218.

Fiorenza, L., Benazzi, S., & Kullmer, O. (2011). Para-masticatory wear facets and their functional significance in hunter–gatherer maxillary molars. *Journal of Archaeological Science*, *38*(9), 2182–2189.

Fiorenza, L., Benazzi, S., Kullmer, O., Zampirolo, G., Mazurier, A., Zanolli, C., & Macchiarelli, R. (2019). Dental macrowear and cortical bone distribution of the Neanderthal mandible from Regourdou (Dordogne, southwestern France). *Journal of Human Evolution*, *132*, 174–188.

Fiorenza, L., Benazzi, S., Oxilia, G., & Kullmer, O. (2018). Functional relationship between dental microwear and diet in late Pleistocene and recent modern human populations. *International Journal of Osteoarchaeology*, *28*, 153–161.

Fiorenza, L., Benazzi, S., Tausch, J., Kullmer, O., Bromage, T. G., & Schrenk, F. (2011). Molar macrowear reveals Neanderthal eco-geographical dietary variation. *PLoS One*, *6*, e14769.

Fiorenza, L., Benazzi, S., Viola, B., Kullmer, O., & Schrenk, F. (2011). Relationship between cusp size and occlusal wear pattern in Neanderthal and Homo sapiens first maxillary molars. *Anatomical Record*, *294*, 453–461.

Fiorenza, L., Habashi, W., Moggi-Cecchi, J., Benazzi, S., & Sarig, R. (2023). Relationship between interproximal and occlusal wear in Australopithecus africanus and Neanderthal molars. *Journal of Human Evolution*, *183*, 103423.

Fiorenza, L., & Kullmer, O. (2013). Dental wear and cultural behavior in middle Paleolithic humans from the near east: Neanderthal nonmasticatory tooth Wear. *American Journal of Physical Anthropology*, *152*, 107–117.

Fiorenza, L., & Kullmer, O. (2016). Occlusion in an adult male gorilla with a supernumerary maxillary premolar. *International Journal of Primatology*, *37*, 762–777.

Fiorenza, L., Nguyen, H. N., & Benazzi, S. (2015). Stress distribution and molar macrowear in Pongo pygmaeus: A new approach through finite element and occlusal fingerprint analyses. *Human Evolution*, *30*, 215–226.

Fisher, N. I. (1993). *Statistical analysis of circular data*. Cambridge University Press.

Friess, M. (2012). Scratching the surface? The use of surface scanning in physical and paleoanthropology. *Journal of Anthropological Sciences*, *90*, 1–25.

Gómez-Robles, A., Bermúdez de Castro, J. M., Martinón-Torres, M., & Prado-Simón, L. (2011). Crown size and cusp proportions in Homo antecessor upper first molars. A comment on quam et al. 2009. *Journal of Anatomy*, *218*, 258–262.

Gómez-Robles, A., Bermúdez de Castro, J. M., Martinón-Torres, M., Prado-Simón, L., & Arsuaga, J. L. (2015). A geometric morphometric analysis of hominin lower molars: Evolutionary implications and overview of postcanine dental variation. *Journal of Human Evolution*, *82*, 34–50.

Grine, F. E., Mongle, C. S., Kollmer, W., Romanos, G., Du Plessis, A., Maureille, B., & Braga, J. (2023). Hypercementosis in late Pleistocene Homo sapiens fossils from Klasies River Main site, South Africa. *Archives of Oral Biology*, *149*, 105664.

Hammer, Ø., & Harper, D. A. (2006). *Paleontological data analysis*. Blackwell Publishing.

Hardy, K., Buckley, S., Collins, M. J., Estalrrich, A., Brothwell, D., Copeland, L., Garía-Tabernero, A., García-Vargas, S., de la Rasilla, M., Lalueza-Fox, C., Huget, R., Bastir, M., Santamaría, D., Mdella, M., Wilson, J., Fernández Cortes, Á., & Rosas, A. (2012). Neanderthal medics? Evidence for food, cooking, and medicinal plants entrapped in dental calculus. *Naturwissenschaften*, *99*, 617–626.

Harty, T., Berthaume, M. A., Bortolini, E., Evans, A. R., Galbany, J., Guy, F., Kullmer, O., Lazzari, V., Romero, A., & Fiorenza, L. (2022). Dental macrowear reveals ecological diversity of gorilla spp. *Scientific Reports*, *12*, 9203.

Henry, A. G., Brooks, A. S., & Piperno, D. R. (2011). Microfossils in calculus demonstrate consumption of plants and cooked foods in Neanderthal diets (Shanidar III, Iraq; spy I and II, Belgium). *Proceedings of the National Academy of Sciences*, *108*, 486–491.

Hillson, S. (2001). Recording dental caries in archaeological human remains. *International Journal of Osteoarchaeology*, *11*, 249–289.

Hillson, S. (2003). *Dental anthropology*. Cambridge University Press.

Ho, S. P., Balooch, M., Goodies, H. E., Marshall, G. W., & Marshall, S. J. (2004). Ultrastructure and nanomechanical properties of cementum dentin junction. *Journal of Biomedical Materials Research*, *68*, 343–351.

Ho, S. P., Kurylo, M. P., Fong, T. K., Lee, S. S., Wagner, H. D., Ryder, M. I., & Marshall, G. W. (2010). The biomechanical characteristics of the bone-periodontal ligament-cementum complex. *Biomaterials*, *31*, 6635–6646.

Ho, S. P., Marshall, S. J., Ryder, M. I., & Marshall, G. W. (2007). The tooth attachment mechanism defined by structure, chemical composition and mechanical properties of collagen fibers in the periodontium. *Biomaterials*, *28*, 5238–5245.

Hylander, W. L. (1979a). The functional significance of primate mandibular form. *Journal of Morphology*, *160*, 223–239.

Hylander, W. L. (1979b). An experimental analysis of temporomandibular joint reaction force in macaques. *American Journal of Physical Anthropology*, *51*(3), 433–456.

Hylander, W. L. (1983). Mechanical properties of food and recruitment of masseter force. *Journal of Dental Research*, *62*, 297.

Hylander, W. L., & Crompton, A. W. (1986). Jaw movements and patterns of mandibular bone strain during mastication in the monkey Macaca fascicularis. *Archives of Oral Biology*, *31*(12), 841–848.

Ichim, I., Kieser, J. A., & Swain, M. V. (2007). Functional significance of strain distribution in the human mandible under masticatory load: Numerical predictions. *Archives of Oral Biology*, *52*(5), 465–473.

Janis, C. M. (1990). The correlation between diet and dental wear in herbivorous mammals, and its relationship to the determination of diets of extinct species. In A. J. Boucot (Ed.), *Evolutionary paleobiology of behavior and coevolution*. Elsevier Science.

Jaouen, K., Villalba-Mouco, V., Smith, G. M., Trost, M., Leichliter, J., Lüdecke, T., Mejean, P., Mandrou, S., Chmeleff, J., Guiserix, D., Bourgon, N., Blasco, F., Mendes Cardoso, J., Duquenoy, C., Moubtahij, Z., Salazar-García, D., Richards, M., Tutken, T., Hublin, J.-J., … Montes, L. (2022). A Neandertal dietary conundrum: Insights provided by tooth enamel Zn isotopes from Gabasa, Spain. *Proceedings of the National Academy of Sciences*, *119*, e2109315119.

Kay, R. F. (1975a). Allometry and early hominids. *Science*, *189*, 63.

Kay, R. F. (1975b). The functional adaptations of primate molar teeth. *American Journal of Physical Anthropology*, *43*, 195–216.

Kay, R. F., & Hiiemae, K. M. (1974). Jaw movement and tooth use in recent and fossil primates. *American Journal of Physical Anthropology*, *40*, 227–256.

Khamnei, S., Sadat-Ebrahimi, S. R., Salarilak, S., Oskoee, S. S., Houshyar, Y., Shakouri, S. K., Salekzamani, Y., & Zamanlu, M. (2019). Manifestation of hemispheric laterality in chewing side preference and handedness. *BioImpacts: BI*, *9*, 189–193.

Kieser, J. A. (1990). *Human adult odontometrics: The study of variation in adult tooth size*. Cambridge University Press.

Krishnan, V., & Davidovitch, Z. (2009). On a path to unfolding the biological mechanisms of orthodontic tooth movement. *Journal of Dental Research*, *88*, 597–608.

Kullmer, O., Benazzi, S., Fiorenza, L., Schulz, D., Bacso, S., & Winzen, O. (2009). Technical note: Occlusal fingerprint analysis: Quantification of tooth wear pattern. *American Journal of Physical Anthropology*, *139*, 600–605.

Kullmer, O., Menz, U., & Fiorenza, L. (2020). Occlusal fingerprint analysis (OFA) reveal dental occlusal behaviour in primate teeth. In T. Martin & W. von Koenigswald (Eds.), *Mammalian teeth: Form and function* (pp. 25–43). Dr. F. Pfeil.

Lamontagne, P., Al-Tarakemah, Y., & Honkala, E. (2013). Relationship between the preferred chewing side and the angulation of anterior tooth guidance. *Medical Principles and Practice*, *22*, 545–549.

Le Cabec, A., Gunz, P., Kupczik, K., Braga, J., & Hublin, J. J. (2013). Anterior tooth root morphology and size in Neanderthals: Taxonomic and functional implications. *Journal of Human Evolution*, *64*(3), 169–193.

Maier, W., & Schneck, G. (1981). Konstruktionsmorphologische Untersuchungen am Gebib der hominoiden Primaten. *Zeitschrift für Morphologie Und Anthropologie*, *72*, 127–169.

Martinón-Torres, M., Martín-Francés, L., Gracia, A., Olejniczak, A., Prado-Simón, L., Gómez-Robles, A., Lapresa, M., Carbonell, E., Arsuaga, J. L., & Bermúdez de Castro, J. M. (2011). Early Pleistocene human mandible from Sima del Elefante (TE) cave site in sierra de Atapuerca (Spain): A palaeopathological study. *Journal of Human Evolution*, *61*, 1–11.

Martinón-Torres, M., Spěváčková, P., Gracia-Téllez, A., Martínez, I., Bruner, E., Arsuaga, J. L., & Bermúdez de Castro, J. M. (2013). Morphometric analysis of molars in a M iddle P leistocene population shows a mosaic of 'modern'and N eanderthal features. *Journal of Anatomy*, *223*, 353–363.

Molnar, S. (1972). Tooth wear and culture: A survey of tooth functions among some prehistoric populations. *Current Anthropology*, *13*, 511–515.

Morgenthal, A., Zaslansky, P., & Fleck, C. (2021). Cementum thickening leads to lower whole tooth mobility and recuced root stress: An *in silico* study on aging effects during mastication. *Journal of Structural Biology*, *213*, 107726.

Naito, Y. I., Chikaraishi, Y., Drucker, D. G., Ohkouchi, N., Semal, P., Wißing, C., & Bocherens, H. (2016). Ecological niche of Neanderthals from spy cave revealed by nitrogen isotopes of individual amino acids in collagen. *Journal of Human Evolution*, *93*, 82–90.

Nanci, A. (2007). *Ten Cate's oral histology: Development, structure, and function*. Mosby, Inc., and affiliates of Elsevier Inc.

Nanci, A., & Bosshardt, D. D. (2000). Structure of periodontal tissue in health and disease. *Periodontology*, *40*(11), 28.

Nicholson, C. M. (2017). Eemian paleoclimate zones and Neanderthal landscape-use: A GIS model of settlement patterning during the last interglacial. *Quaternary International*, *438B*, 144e157.

Nicklisch, N., Hinrichs, C., Palaske, L., Vach, W., & Alt, K. W. (2023). Variability in human tooth cementum thickness reflecting functional processes. *Journal of Periodontal Research*, *00*, 1–12.

Olejniczak, A. J., Smith, T. M., Feeney, R. N. M., Macchiarelli, R., Mazurier, A., Bondioli, L., Rosas, A., Fortea, J., de la Rasilla, M., Garcia-Tabernero, A., Radovcic, J., Skinner, M. M., Toussaint, M., & Hublin, J. J. (2008). Dental tissue proportions and enamel thickness in Neandertal and modern human molars. *Journal of Human Evolution*, *55*, 12–23.

Oxilia, G., Bortolini, E., Martini, S., Papini, A., Boggioni, M., Buti, L., Figus, C., Sorrentino, R., Townsend, G., John, K., Fiorenza, L., Cristiani, E., Kullmer, O., Moggi-Cecchi, J., & Benazzi, S. (2018). The physiological linkage between molar inclination and dental macrowear pattern. *American Journal of Physical Anthropology*, *166*, 941–951.

Patriquin, M. L. (2013). The relationship between masticatory stress and prognathism: A finite element and morphometric study. [Ph.D. dissertation]. University of Pretoria, Africa.

Plavcan, J. M., Meyer, V., Hammond, A. S., Couture, C., Madelaine, S., Holliday, T. W., Maureille, B., Ward, C. V., & Trinkaus, E. (2014). The Regourdou 1 Neandertal body size. *Comptes Rendus Palevol*, *13*, 747e754.

Rak, Y. (1986). The Neanderthal: A new look at an old face. *Journal of Human Evolution*, *15*, 151–164.

Rego, E. B., Inubushi, T., Kawazoe, A., Miyauchi, M., Tanaka, E., Takata, T., & Tanne, K. (2011). Effect of PGE2 induced by compressive and tensile stresses on cementoblast differentiation in vitro. *Archives of Oral Biology*, *56*, 1238–1246.

Ren, L. M., Wang, W. X., Takao, Y., & Chen, Z. X. (2010). Effects of cementum-dentine junction and cementum on the mechanical response of tooth supporting structure. *Journal of Dentistry*, *38*, 882–891.

Richards, M. P., & Trinkaus, E. (2009). Isotopic evidence for the diets of European Neanderthals and early modern humans. *Proceedings of the National Academy of Sciences*, *106*, 16034–16039.

Rios, H. F., Ma, D., Xie, Y., Giannobile, W. V., Bonewald, L. F., Conway, S. J., & Feng, J. Q. (2008). Periostin is essential for the integrity and function of the periodontal ligament during occlusal loading in mice. *Journal of Periodontology*, *79*, 1480–1490.

Robson, R. M. (1994). A multi-component rose diagram. *Journal of Structural Geology*, *16*, 1039–1040.

Salazar-García, D. C., Power, R. C., Serra, A. S., Villaverde, V., Walker, M. J., & Henry, A. G. (2013). Neanderthal diets in central and southeastern Mediterranean Iberia. *Quaternary International*, *318*, 3–18.

Shaw, A. M., Sameshima, G. T., & Vu, H. V. (2004). Mechanical stress generated by orthodontic forces on apical root cementum: A finite element model. *Orthodontics & Craniofacial Research*, *7*, 98–107.

Skinner, M. M., Evans, A., Smith, T., Jernvall, J., Tafforeau, P., Kupczik, K., Olejniczak, A. J., Rosas, A., Radovcic, J., Thackeray, J. F., Toussaint, M., & Hublin, J. J. (2010). Brief communication: Contributions of enamel-dentine junction shape and enamel deposition to primate molar crown complexity. *American Journal of Physical Anthropology: The Official Publication of the American Association of Physical Anthropologists*, *142*, 157–163.

Smith, B. H. (1984). Patterns of molar wear in hunter-gatherers and agriculturists. *American Journal of Physical Anthropology*, *63*, 39–56.

Smith, F. H. (1982). Upper Pleistocene hominid evolution in south–Central Europe: A review of the evidence and analysis of trends. *Current Anthropology*, *23*, 667–703.

Stringer, C., & Gamble, C. (1993). *In search of the Neanderthals*. Thames and Hudson Ltd.

Tacail, T., Martin, J. E., Arnaud-Godet, F., Thackeray, J. F., Cerling, T. E., Braga, J., & Balter, V. (2019). Calcium isotopic patterns in enamel reflect different nursing behaviors among south African early hominins. *Science Advances*, *5*, eaax3250.

Trinkaus, E. (1992). Morphological contrasts between the near eastern Qafzeh-Skhul and late archaic human samples: Grounds for behavioural difference? In T. Akazawa, K. Aoki, & T. Kimura (Eds.), *The evolution and dispersal of modern humans in Asia*. Tokyo, Hokusen-sha.

van Andel, T. H., & Tzedakis, P. C. (1996). Paleolithic landscapes of Europe and environs, 150,000-25,000 years ago: An overview. *Quaternary Science Review*, *15*, 481–500.

Vandermeersch, B., & Trinkaus, E. (1995). The postcranial remains of the Regourdou 1 Neandertal: The shoulder and arm remains. *Journal of Human Evolution*, *28*, 439e476.

Wolpoff, M. H. (1971). *Metric trends in hominid dental evolution*. Press of Case Western Reserve University.

Zanolli, C., Genochio, L., Tournepiche, J. F., Mazurier, A., & Macchiarelli, R. (2020). The Neanderthal mandible BD 1 from La chaise-de-Vouthon Abri bourgeois-Delaunay (Charente, southwestern France, OIS 5e). Dental tissue proportions, cortical bone distribution and endostructural asymmetry. *Paleo*, *30*, 346–359.

Zanolli, C., Kullmer, O., Kelley, J., Bacon, A. M., Demeter, F., Dumoncel, J., Fiorenza, L., Grine, F. E., Hublin, J.-J., Nguyen, A. T., Nguyen, T. M. H., Pan, L., Schillinger, B., Schrenk, F., Skinner, M., Ji, X., & Macchiarelli, R. (2019). Evidence for increased hominid diversity in the early to middle Pleistocene of Indonesia. *Nature Ecology & Evolution*, *3*, 755–764.

Zhou, J., Zhao, Y. F., Xia, C. Y., & Jiang, L. (2012). Periodontitis with hypercementosis: Report of a case and discussion of possible aetiologic factors. *Australian Dental Journal*, *57*, 511–514.

SUPPORTING INFORMATION

Additional supporting information can be found online in the Supporting Information section at the end of this article.

How to cite this article: Hernaiz-García, M., Zanolli, C., Martín-Francés, L., Mazurier, A., Benazzi, S., Sarig, R., Fu, J., Kullmer, O., & Fiorenza, L. (2024). Masticatory habits of the adult Neanderthal individual BD 1 from La Chaise-de-Vouthon (France). *American Journal of Biological Anthropology*, *184*(1), e24926. https://doi.org/10.1002/ajpa.24926